Double-layer structural design of dielectric ordered mesoporous carbon/paraffin composites for microwave absorption

**Hongjing Wu · Liuding Wang · Shaoli Guo ·
Zhongyuan Shen**

Abstract Microwave absorbing materials composed of ordered mesoporous carbon (OMC) as absorbent and paraffin as matrix were prepared, and their electromagnetic and microwave absorbing properties could be tuned by changing the weight fraction of OMC at 2–18 GHz. The minimum reflection loss (*RL*) value reached −9.3 dB at 8.0 GHz and the absorption range with *RL* lower than −5 dB was obtained at 5.8–14.4 GHz for a single-layer absorber filled with 1.98 wt.% OMC at 3.0 mm. If a double-layer structure was adopted, the total thickness of the absorber could be reduced below 2.0 mm and the effective absorption range (*RL* < −10 dB) could be obtained at 8.9–14.3 GHz with a minimal *RL* of −28.5 dB at 10.6 GHz. This work demonstrated that dielectric composites could be used as excellent absorbers by adopting reasonable multilayer structures.

1 Introduction

With the rocketing development of information technology, the problem of electromagnetic interference (EMI) becomes more serious due to the broad application of electromagnetic (EM) waves at high frequencies [1]. The misoperation of precise electronic equipment and leaks of secret information may occur due to the leakage of EM waves [2, 3]. EMI shielding materials can effectively prevent the leakage of EM waves. However, in military applications, particularly in an antiradar system the used materials should have a strong absorbing effect. Thus, EM wave absorbers with

wider absorption bandwidths and better absorption properties become more and more important.

Recently, conducting carbon materials especially ordered mesoporous carbon (OMC) have been widely used as EMI shielding [4] or microwave-absorbing [5, 6] materials when being added into the ceramic or epoxy resin matrix. He et al. [5] prepared ordered meso-C-Al$_2$O$_3$ nanocomposites via the evaporation-induced self-assembly method. The bandwidth below −10 dB was 7.4 GHz with a thickness of 3.0 mm at 0.5–18 GHz. Meanwhile, they prepared a series of meso-C-SiO$_2$-Fe nanocomposites by the same approach and found the minimum reflection loss (*RL*) value reaching −34.4 dB at 13.1 GHz [6]. It indicated that compounding different types of absorbents could remarkably improve the absorption efficiency and effective absorbing bands of the absorbers [7]. However, single-layer absorbers have only good absorption properties within a very narrow frequency range due to the less variable parameters of its design [8]. Besides, it is quite difficult to improve the absorption efficiency and bandwidths of the absorbers by only adding optimized absorbents. Therefore, multilayer absorbers have been devised by superimposing a variety of absorbents to obtain wider absorption bandwidths and smaller *RL* values [9]. For example, Qing et al. [10] prepared double-layer absorbers by adopting a matching layer filled with 50 % BaTiO$_3$ and an absorption layer composed of 60 % BaTiO$_3$ and 20 % carbonyl ion (CI). The absorption range with *RL* lower than −10 dB could be obtained at 10.8–14.8 GHz and the minimum *RL* value of −59 dB could be achieved at 12.5 GHz. In the double-layer absorber, the matching layer with good transmission capacity firstly achieved a good impedance matching, and then the absorption layer could achieve an excellent absorption capacity.

In this paper, the EM properties of the microwave absorbing materials at 2–18 GHz were reported, based on different

H. Wu (✉) · L. Wang · S. Guo · Z. Shen
Department of Applied Physics, Northwestern Polytechnical
University, Xi'an 710072, P.R. China
e-mail: wuhongjing@mail.nwpu.edu.cn
Fax: +86-29-88431664

weight fractions of OMC within paraffin matrix. Double-layer microwave absorption coatings were fabricated using different OMC/paraffin composites in the matching layer and absorption layer, respectively. The *RL* of the double-layer absorber was theoretically predicted based on the model of double-layer absorbers and compared with that of single-layer absorbers. It suggested that the excellent microwave absorbing properties was mainly originated from the dielectric loss of OMC in the optimal designed double-layer microwave absorbing materials.

2 Experimental

2.1 Materials and preparation

A high-quality mesoporous silica (i.e., SBA-15) sample was prepared by means of the triblock copolymer, $EO_{20}PO_{70}EO_{20}$ (Pluronic 123, BASF), as the surfactant and tetraethyl orthosilicate (TEOS, 98 %, Acros) as the silica source, following the synthesis procedures reported by Zhao et al. [11]. Typically, 8.8 g of TEOS was added into 120 ml of 1.6 M HCl containing 4 g of Pluronic 123 at 35 °C. This gel was stirred continuously for 24 h and then was crystallized in a Teflon-lined autoclave at 100 °C for 12 h. The product was filtered, dried, and calcined at 500 °C for 5 h.

Then the calcined SBA-15 (1 g) was impregnated with a solution obtained by dissolving 1.25 g of sucrose and 0.14 g of H_2SO_4 in 5 g of water [12]. The mixture was placed in a drying oven at 80 °C for 6 h, and subsequently the oven temperature was increased to 160 °C and maintained there for 6 h. After the treatment in the oven, the sample turned dark brown. The pretreated sample was treated again at 80 and 160 °C after the addition of 0.8 g of sucrose, 0.09 g of H_2SO_4 and 5 g of H_2O. The carbonization was completed by pyrolysis at 900 °C under N_2. The

OMC/paraffin composite samples were prepared by ultrasonic agitation to mix a certain weight fraction of OMC with paraffin. The use of the paraffin as the matrix is because it is a microwave-transparent material. So the microwave absorption properties of the OMC/paraffin composites mainly depend on the content of OMC absorbent. The paraffin composites filled with 1.98 wt.%, 2.99 wt.%, 4.70 wt.%, and 5.69 wt.% weight fractions of OMC are denoted as 1.98OMC, 2.99OMC, 4.70OMC, and 5.69OMC, respectively.

2.2 Characterization

Transmission electron microscopy (TEM) images were taken on a JEOL JEM-2100 electron microscope operating at 200 kV. The synthesized OMC was characterized by low-angle X-ray diffraction (XRD) on a Rigaku D/MAX diffractometer (Cu Kα radiation, $\lambda = 1.5406$ Å). The BET specific surface area of the OMC was measured by nitrogen adsorption at -196 °C using a Builder SSA-4200 analyzer. The prepared powder was pressed into a toroid with an outer diameter of 7.0 mm, inner diameter of 3.04 mm, and thickness of 3.0 mm. The complex permittivity and permeability data of OMC/paraffin composites were measured using a HP vector network analyzer (HP 8720B) at 2–18 GHz.

3 Results and discussion

3.1 Morphology

A detailed structural characterization is revealed by TEM images as shown in Fig. 1. It can be clearly seen that the ordered mesoporous structure of the OMC is perfectly

Fig. 1 TEM images of ordered mesoporous carbon: (**a**) overview and (**b**) larger magnification along the [110] directions
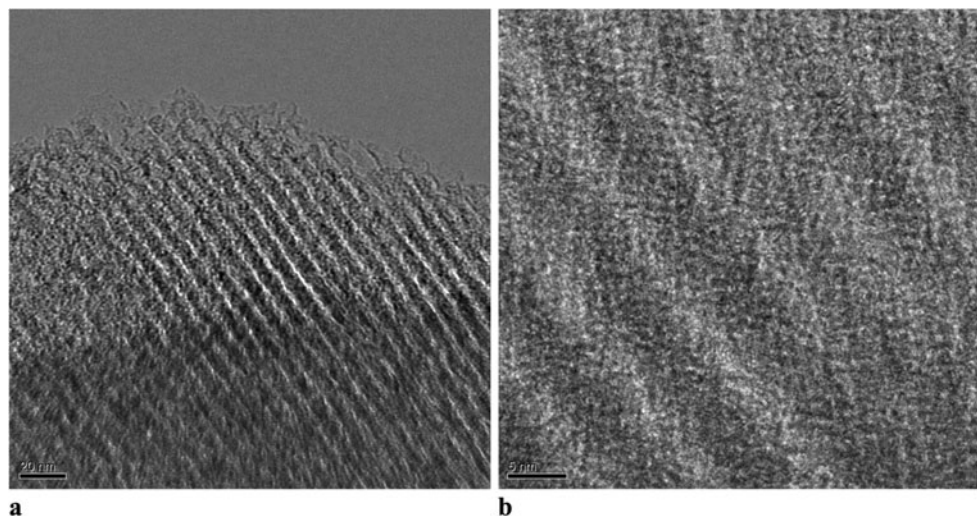
formed, which exhibits a reverse hexagonal structure of ordered mesoporous silica (SBA-15) [12]. The HRTEM images show that the carbon nanorods in OMC are 5.9 in diameter, the centers of adjacent rods are 8.3 nm apart, and the pore size is 2.4 nm. The unique nanostructure of OMC nanowire arrays, with a high specific surface and more dangling bonds, is prone to interface polarization and plays a significant role in its attenuation of microwave by multiscattering and reflecting.

The low-angle XRD pattern of OMC (Fig. 2) shows a relatively sharp peak at $2\theta = 0.95°$ with two relatively weak peaks at around 2θ of $1.70°$ and $2.00°$, which can be indexed to (100), (110), and (200) diffractions of the *p6mm* symmetry, respectively [12]. The intense (100) peak reflects a *d*-spacing of 9.3 nm corresponding to a unit-cell constant $a_0 = 10.74$ nm.

Figure 3 shows the nitrogen adsorption-desorption isotherm and pore-size distribution of OMC. The carbon material presents an isotherm characteristic of mesoporous material with a hysteresis loop of type IV, suggesting its uniform cylindrical pores (Fig. 3a). The OMC has a BET surface area of 123 $m^2\,g^{-1}$ and a pore volume of 0.19 $cm^3\,g^{-1}$.

Fig. 2 Low-angle XRD pattern of OMC
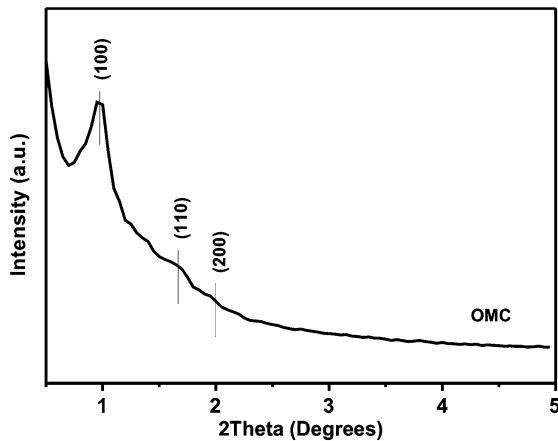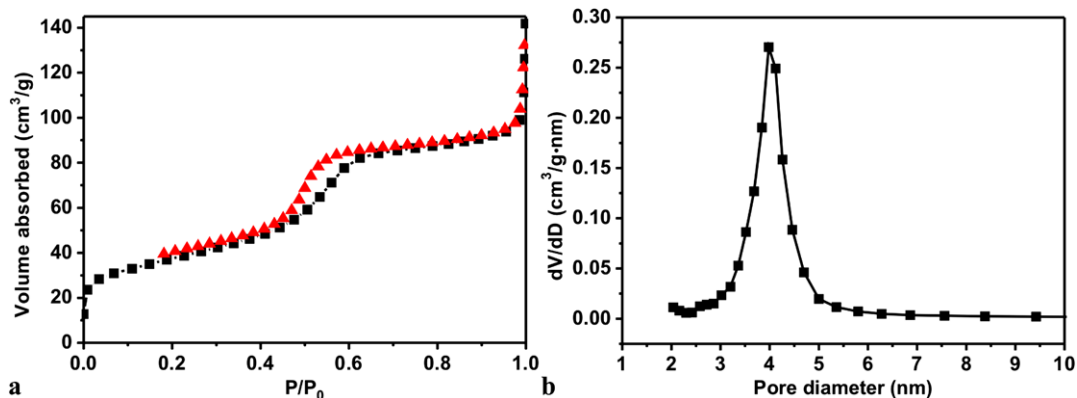
In Fig. 3b, the pore-size distribution obtained for OMC from N_2 desorption indicates that the OMC is mostly nanoporous with quite narrow pore-size distribution centered at 4.0 nm. The pore width of OMC determined from nitrogen desorption is a bit larger than the HRTEM data because of the void space between hexagonally nanowire arrays.

3.2 EM properties of the OMC/paraffin composites with different weight fractions of OMC

It is well known that interactions between absorbers and electromagnetic field in the microwave frequency band can be expressed by the complex permittivity ($\varepsilon = \varepsilon' - j\varepsilon''$) and complex permeability ($\mu = \mu' - j\mu''$). The real parts (ε' and μ') of complex permittivity and permeability are related to the storage capability of electric and magnetic energy. The imaginary parts (ε'' and μ'') account for the loss energy dissipative mechanisms in the composites.

Figures 4a and 4b shows the complex permittivity spectra of the OMC/paraffin composites as a function of frequency. With the content of OMC increases from 1.98 wt.% to 5.69 wt.%, the real (ε') ascends with increasing frequency at 2–18 GHz as a whole regardless of small difference between 1.98 wt.% and 2.99 wt.% (or between 4.70 wt.% and 5.69 wt.%). Additionally, the imaginary (ε'') permittivity of the composites increases monotonously with increasing weight fraction of OMC. The results can be attributed to the dielectric property and weight fraction of the OMC, and the configuration and internal structure of the paraffin composites [13]. As we all know, with the increase of filler, the composites can form more interfaces between the filler and matrix, and thus the higher complex permittivity can be obtained due to the enhancement of the interfacial polarization and the interactions between the fillers [14, 15]. Qing et al. [13] considered that there were two main contributors for the high complex permittivity of the composites containing multiwall carbon nanotubes (MWCNTs) and CI particles. As the content of the MWCNTs increased the enhance-
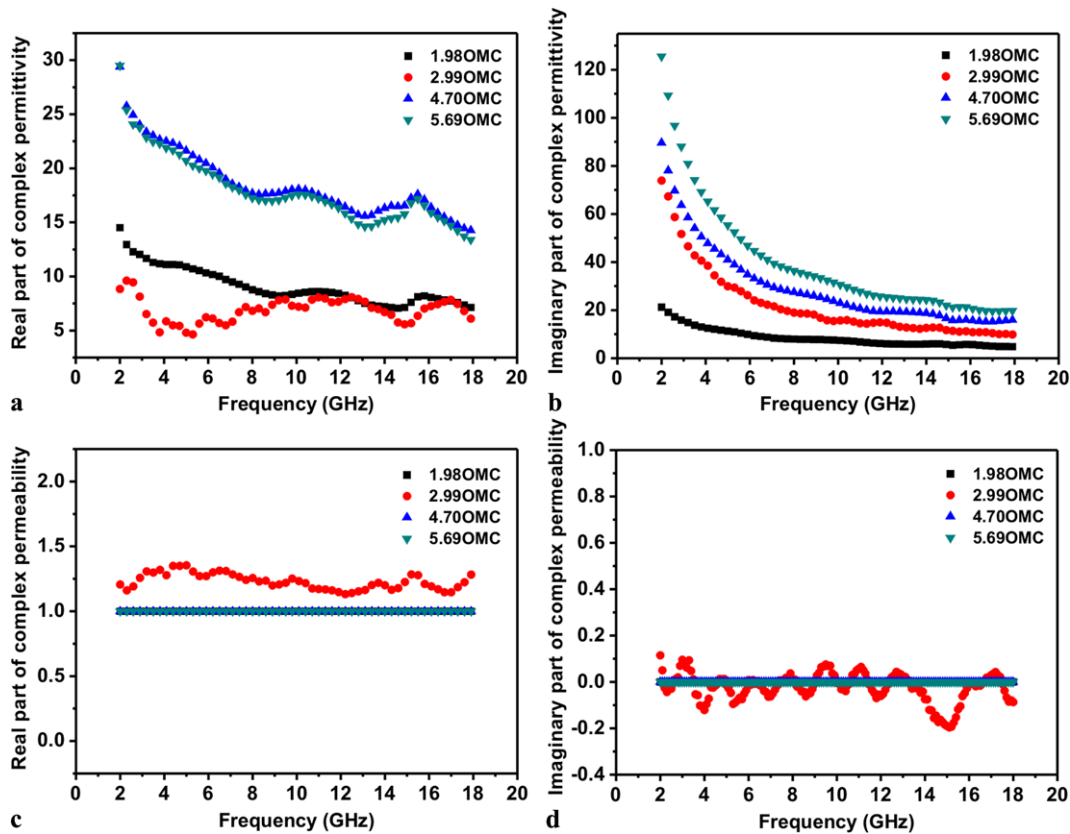

Fig. 3 (**a**) N_2 adsorption-desorption isotherm and (**b**) pore-size distribution at -196 °C for OMC

H. Wu et al.

Fig. 4 (**a** and **b**) The complex permittivity and (**c** and **d**) permeability of the OMC/paraffin composites as a function of the weight content of OMC

ment of interfacial polarization at the MWCNTs/CI particles/resin, interfaces and orientation polarization of MWCNTs and CI particles could contribute to the increase of complex permittivity [15].

Furthermore, the real permittivity (ε') declines as a function of frequency and exhibits a visible frequency-dependent dielectric response, i.e., fluctuations at about 10.5 GHz and 15.5 GHz. The result suggests the existence of a resonance behavior, which can be explained by the effective medium theory developed by Lagarkov and Sarychev [16]. The imaginary permittivity (ε'') shows a general decaying behavior toward higher frequency, which is consistent with the report [17]. This phenomenon is understandable because the polarization of the dielectric dipoles is in phase with the oscillation of the electric field vector of the transverse EM wave, with the increase in frequency [18].

Figures 4c and 4d show the complex permeability of the OMC/paraffin composites. The real (μ') and the imaginary (μ'') permeability are nearly constant ($\mu' \approx 1$ and $\mu'' \approx 0$, respectively) except for the one with 2.99OMC as the absorber, which means that the magnetic loss tangent $\tan\delta_\mu$ of 1.98OMC, 4.70OMC, and 5.69OMC are close to negligibly small ($\tan\delta_\mu = 0$), i.e., the absorbers interact with EM wave without magnetic loss. Hence, the microwave absorbing mechanisms of the OMC/paraffin composites can be associated with (1) resistance loss of conductive OMC, which can attenuate the EM wave; (2) novel nanostructure of hexagonally ordered carbon nanowire arrays of OMC, which can favor microwave absorption by multiscatter and reflection; (3) interfacial polarization and orientation polarization, which can be more easily induced at low frequencies and the interactions between conductive OMC particles can attenuate the EM waves [19].

3.3 Microwave absorption of single-layer microwave absorbers

The theoretical reflection loss of EM waves is calculated from the complex permittivity and permeability according to the transmission line theory. The reflection loss for a single-layer absorber is given by the following equations [20]:

$$RL = 20\log\left|(Z_\text{in} - Z_0)/(Z_\text{in} + Z_0)\right| \tag{1}$$

$$Z_0 = \sqrt{\frac{\mu_0}{\varepsilon_0}} \tag{2}$$

$$Z_\text{in} = Z_0\sqrt{\frac{\mu_r}{\varepsilon_r}}\tanh\left[j\frac{2\pi f d}{c}\sqrt{\mu_r\varepsilon_r}\right] \tag{3}$$
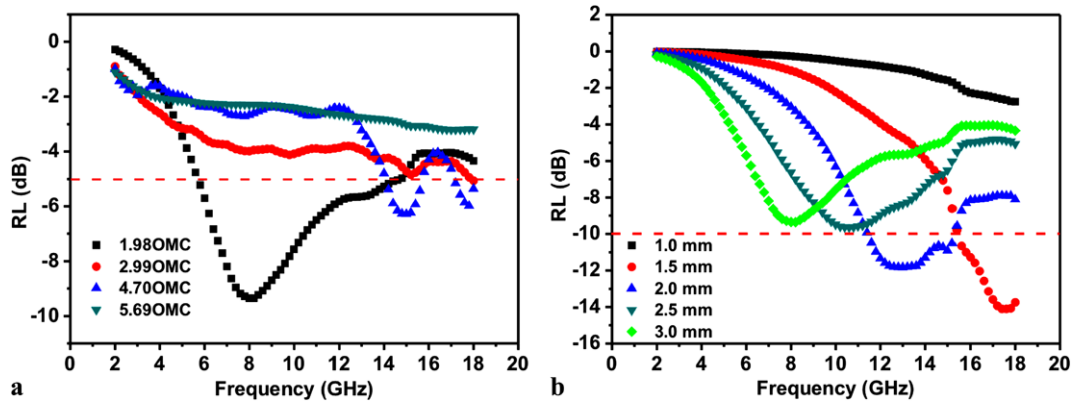
Springer

Fig. 5 The frequency dependence of the reflection loss of (**a**) the composites with a coating thickness of 3.0 mm and (**b**) 1.98OMC with coating thickness from 1.0 to 3.0 mm

where ε_0 and μ_0 are the complex permittivity and permeability of free space, Z_0 is the impedance of free space, Z_{in} is the input impedance of absorber, ε_r and μ_r are the complex permittivity and permeability of the composite, f is the frequency of the EM waves, d is the thickness of an absorber, and c is the velocity of EM waves.

Figure 5a shows the *RL* of the OMC/paraffin composites at 2–18 GHz. The minimum *RL* for the 1.98OMC is measured to be −9.3 dB at 8.0 GHz, and the absorption range with *RL* lower than −5 dB (over 70 % microwave absorption) can be obtained at 5.8–14.4 GHz. However, as increasing the content of OMC, the microwave absorption performances are not good at 2–18 GHz. There is no frequency range with *RL* lower than −5 dB for the 2.99OMC and 5.69OMC, and the effective absorption bandwidths (*RL* < −5 dB) is only 1.8 GHz for 4.70OMC.

The calculated result with different thicknesses of 1.98OMC is shown in Fig. 5b. The minimum *RL* value shifts to the higher frequency range from 8.0 GHz to 17.6 GHz as the thickness decreases from 3.0 to 1.5 mm. In addition, the absorption range with *RL* below −10 dB can be obtained at 11.4–15.4 GHz and 15.4–18 GHz when the coating thicknesses are 2.0 and 1.5 mm, respectively. When the thickness is 1.5 mm, the composite shows strong microwave absorption at high frequencies with a minimal *RL* of −14.1 dB at 17.6 GHz. According to Eqs. (1)–(3), the *RL* of an absorber is determined by the complex permittivity and permeability as well as the thickness of microwave absorbing materials. So, it is implied that we can get higher microwave absorption over a broad frequency range by changing the content of OMC in the coatings to meet different demands. In this paper, the complex permittivity of 1.98OMC is inferior to that of other composites at 2–18 GHz. The input impedance at the surface of the 1.98OMC could be matched to the impedance of the air much better than that of other absorbers with higher content of OMC. Consequently, a double-layer
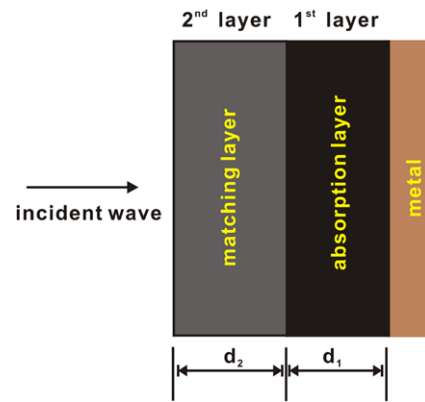

Fig. 6 Structure of proposed double-layer microwave absorbing material

absorber using 1.98OMC as the matching layer and others as the absorption layer may be a promising microwave absorbing material.

3.4 Microwave absorption properties and structural design of double-layer microwave absorbers

For a double-layer absorber composed of the first layer as the load side and second layer as the incident wave side shown in Fig. 6, the *RL* can be calculated by the following equations [20]:

$$Z_{\text{in}(1)} = Z_1 \tanh\left(j(2\pi f d/c)\sqrt{\mu_{1r}\varepsilon_{1r}}\right) \tag{4}$$

$$Z_1 = Z_0\sqrt{\mu_{1r}/\varepsilon_{1r}} \tag{5}$$

$$Z_{\text{in}(2)} = \frac{Z_2(Z_{\text{in}(1)} + Z_2 \tanh(j(2\pi f d/c)\sqrt{\mu_{2r}\varepsilon_{2r}}))}{Z_2 + Z_{\text{in}(1)} \tanh(j(2\pi f d/c)\sqrt{\mu_{2r}\varepsilon_{2r}})} \tag{6}$$

$$Z_2 = Z_0\sqrt{\mu_{2r}/\varepsilon_{2r}} \tag{7}$$

$$RL = 20\log\left|(Z_{\text{in}(2)} - Z_0)/(Z_{\text{in}(2)} + Z_0)\right| \tag{8}$$

where $Z_{\text{in}(1)}$ is the input impedance between the matching layer and the absorption layer, $Z_{\text{in}(2)}$ is the input impedance

between the free space and the absorber interface, Z_0, Z_1, and Z_2 are the characteristic impedance of vacuum, the first and second layer, μ_{1r}, ε_{1r} and μ_{2r}, ε_{2r} are the complex permeability and permittivity of the first and second layer, respectively.

In the following, in order to obtain microwave absorbers with a minimum RL value over a broad frequency range, the double microwave absorbers are designed and the design process encompasses the determination of the optimal choice of the material for each layer and its thickness.

Figure 7 shows the dependence of the RL for the double-layer absorber on the absorption layer when the thickness of the matching layer and absorption layer keep constant (1.0 mm). Values for the minimal of RL decreases from -28 dB to -16 dB, but the location of RL peaks for all composites almost stay unchangeable. It is worth to note that the minimum RL value can be remarkably improved by reducing the difference of weight fraction of OMC between the matching and absorption layers. It is observed that the absorption range with RL under -10 dB can be obtained at 8.9–14.3 GHz by using the 1.98OMC/2.99OMC double-layer absorber. Compared with a single-layer absorber composed of 1.98OMC (3.0 mm, as shown in Fig. 3a), the RL can be greatly enhanced and the total thickness can be reduced (2.0 mm). Microwave absorption properties of a single-layer absorber and different structural double-layer absorbers are compared in Table 1.

Figures 8 and 9 show the effects of the absorption or matching layer thickness on the RL of the 1.98OMC/2.99OMC double-layer absorber, respectively, when the thickness of the matching layer or absorption layer keeps 1.0 mm. As the adsorption layer increases from 0.5 to 2.0 mm (Fig. 6), the minimal RL shifts to the lower frequency range, i.e., from 14.9 GHz to 7.7 GHz and decreases from -28 to -14 dB with increasing absorption layer thickness. It is interesting to note that by changing the thickness of the absorption layer, the minimum RL value declines significantly, but the bandwidths of the RL becomes wider.

On the other hand, if the thickness of the matching layer increases from 0.5 to 2.0 mm (Fig. 7), the minimum RL value increases from -31.4 to -35.5 dB, but the bandwidths of the RL value below -10 dB becomes a bit narrower. If the absorption and matching layer of 1.98OMC/2.99OMC are in reverse order, i.e., 2.99OMC as matching layer and
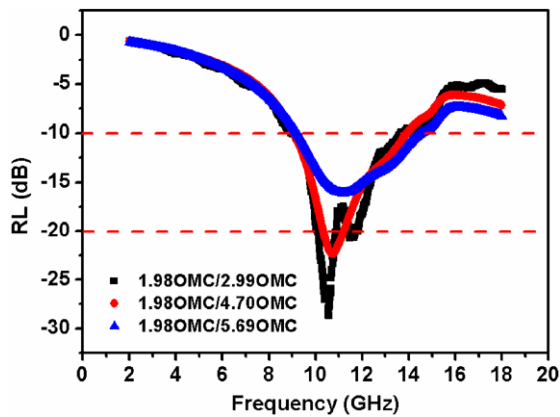
Fig. 7 The RL of double-layer microwave absorber consisted of 1.98OMC as matching layer, and 2.99OMC, 4.70OMC, or 5.69OMC as an absorption layer, respectively
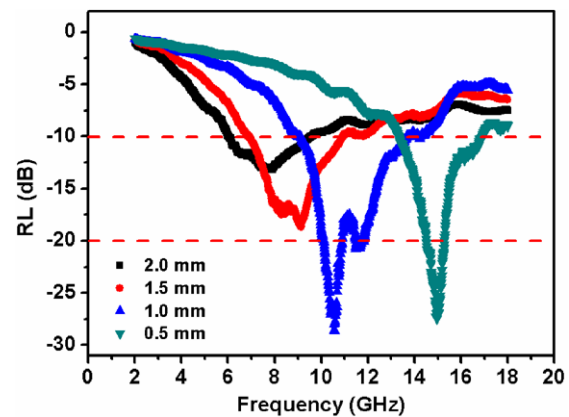
Fig. 8 The RL of 1.98OMC/2.99OMC whose thickness of the matching layer is 1.0 mm and the absorption layer increased from 0.5 to 2.0 mm

Table 1 Composition and detail microwave absorption properties of the designed single-layer and double-layer absorbers

| Structure	Material	Thickness	Minimum RL (dB)	f_m (GHz) (minimum RL)	Bandwidth $RL < -10$ (GHz)	Total thickness (mm)
Single-layer	1.98OMC	3.0	-9.3	8.0	0	3.0
Double-layer	1.98OMC/2.99OMC	$1.0 + 1.0$	-28.5	10.6	8.9–14.3	2.0
Double-layer	1.98OMC/4.70OMC	$1.0 + 1.0$	-22.3	10.7	9.0–14.0	2.0
Double-layer	1.98OMC/5.69OMC	$1.0 + 1.0$	-16.1	11.2	9.1–14.7	2.0
Double-layer	1.98OMC/2.99OMC	$2.0 + 1.0$	-35.5	6.2	4.9–7.6	3.0
Double-layer	1.98OMC/2.99OMC	$1.5 + 1.0$	-34.1	8.2	6.4–9.5	2.5
Double-layer	1.98OMC/2.99OMC	$0.5 + 1.0$	-31.4	15.8	13.2–18	1.5
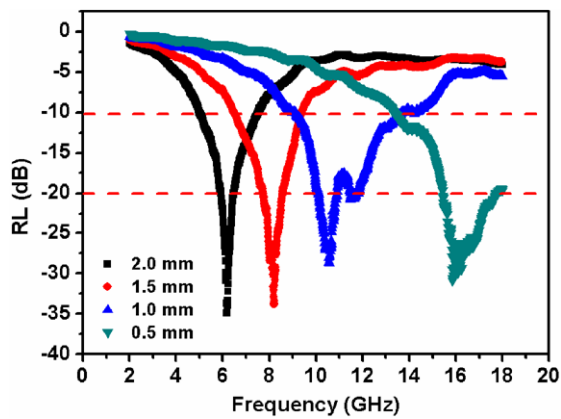
Fig. 9 The *RL* of 1.98OMC/2.99OMC whose thickness of the absorption layer is 1.0 mm and the matching layer increased from 0.5 to 2.0 mm
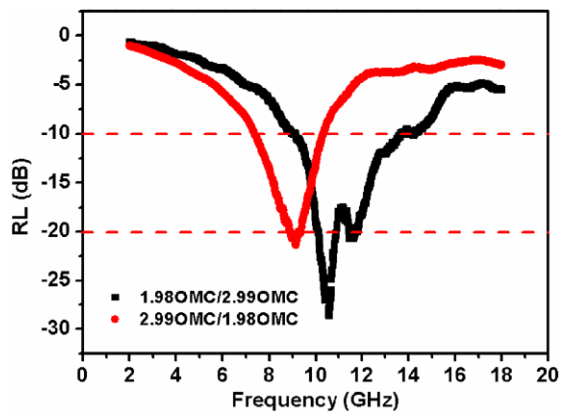

Fig. 10 The *RL* of 1.98OMC/2.99OMC and 2.99OMC/1.98OMC, respectively

1.98OMC as absorption layer, respectively, the minimal *RL* decreases and the bandwidths of the *RL* below −10 dB becomes narrower obviously as shown in Fig. 10. Based on the above results, the structural design including the optimal choice and respective thickness as well as the order of each layer are extremely important for multilayer microwave absorbing materials.

It is evident that by adopting a double-layer structural microwave absorber coating, not only the microwave absorption properties can be enhanced significantly, but also the total layer thickness can be reduced as compared with a single-layer absorber. In fact, the dielectric loss of the matching layer made of 1.98OMC is low, and its impedance is close to the air, thus the EM wave can enter the matching layer as much as possible [21]. Moreover, the absorption layer composed of higher content of OMC possesses relatively higher dielectric loss, and the EM wave in the composites can be effectively attenuated. The two keys (i) the impedance matching characteristic and (ii) the attenuation characteristic can

be well satisfied by the double-layer absorbers for achieving excellent microwave absorbing materials.

4 Conclusions

The electromagnetic and microwave absorbing properties of the single-layer OMC/paraffin composites were studied as a function of frequency and weight fraction of OMC. The complex permittivity of the composites decreased with increasing frequency and ascended gradually with increasing the weight fraction of OMC as a whole. By changing the content of OMC in the composites, we can tune the dielectric loss of the absorber, and the results inspired us by designing a double-layer microwave absorbing material. For the single-layer composite filled with 1.98OMC the absorption range with *RL* under −5 dB can be obtained at 5.8–14.4 GHz with a thickness of 3.0 mm. However, the effective absorption range (*RL* < −10 dB) can be achieved by a double-layer absorber, i.e., 1.98OMC/2.99OMC, at 8.9–14.3 GHz and the minimal *RL* of −28.5 dB can be obtained at 10.6 GHz with the thickness of 2.0 mm. This work suggests that the dielectric OMC-based composites can be used as excellent microwave absorbers with broader bandwidths and thinner matching thickness by adopting double-layer structural design.

References

1. Y.C. Qing, W.C. Zhou, S. Jia, F. Luo, D.M. Zhu, Appl. Phys. A **100**, 1177 (2010)
2. M.S. Cao, R. Qin, C.J. Qiu, J. Zhu, Mater. Des. **24**, 391 (2003)
3. S.S. Kim, S.T. Kim, Y.C. Yoon, K.S. Lee, Appl. Phys. Lett. **97**, 10F905 (2005)
4. J.C. Wang, C.S. Xiang, Q. Liu, Y.B. Pan, J.K. Guo, Adv. Funct. Mater. **18**, 2995 (2008)
5. T. Wang, J.P. He, J.H. Zhou, X.C. Ding, J.Q. Zhao, S.C. Wu, Y.X. Guo, Microporous Mesoporous Mater. **134**, 58 (2010)
6. J.H. Zhou, J.P. He, G.X. Li, T. Wang, D. Sun, X.C. Ding, J.Q. Zhao, S.C. Wu, J. Phys. Chem. C **114**, 7611 (2010)
7. Y. Li, C.X. Chen, X.Y. Pan, Y.W. Ni, S. Zhang, J. Huang, D. Chen, Y.F. Zhang, Physica B **404**, 1343 (2009)
8. M. Wang, Y.P. Duan, S.H. Liu, X.G. Li, Z.J. Ji, J. Magn. Magn. Mater. **321**, 3442 (2009)
9. M.S. Cao, J. Zhu, J. Yuan, T.F. Zhang, Z.H. Peng, Z.J. Gao, G. Xiao, S.M. Qin, Mater. Des. **23**, 557 (2002)
10. Y.C. Qing, W.C. Zhou, F. Luo, D.M. Zhu, J. Magn. Magn. Mater. **323**, 600 (2011)
11. D.Y. Zhao, J.L. Feng, Q.S. Huo, N. Melosh, G.H. Fredrickson, B.F. Chmelka, G.D. Stucky, Science **279**, 548 (1998)
12. S. Jun, H. Joo, R. Ryoo, M. Kruk, M. Jaroniec, Z. Liu, T. Ohsuna, O. Terasaki, J. Am. Chem. Soc. **122**, 10712 (2000)

13. Y.C. Qing, W.C. Zhou, F. Luo, D.M. Zhu, Carbon **48**, 4074 (2010)
14. Z. Dang, Y. Shen, L. Fan, N. Cai, C. Nan, S. Zhao, J. Appl. Phys. **93**, 5543 (2003)
15. B. Zhang, Y. Feng, J. Xiong, Y. Yang, H. Lu, IEEE Trans. Magn. **42**, 1778 (2006)
16. A.N. Lagarkov, A.K. Sarychev, Phys. Rev. B **53**, 6318 (1996)
17. R.C. Che, L.M. Peng, X.F. Duan, Q. Chen, X.L. Liang, Adv. Mater. **16**, 401 (2004)
18. G.Z. Shen, M. Xu, Z. Xu, Mater. Chem. Phys. **105**, 268 (2007)
19. Y.P. Duan, Y. Yang, H. Ma, S.H. Liu, X.D. Cui, H.F. Chen, J. Phys. D, Appl. Phys. **41**, 125403 (2008)
20. E. Michielssen, J.M. Sager, S. Ranjithan, R. Mittra, IEEE Trans. Microw. Theory Tech. **41**, 1024 (1993)
21. Y.B. Feng, T. Qiu, C.Y. Shen, J. Magn. Magn. Mater. **318**, 8 (2007)